EVALUATION OF HYDROGEN PERMEABILITY ON NIO-DOPED ALUMINA BASED NICKEL COMPOSITE MEMBRANE

B. Y. Son, Y. S. Kim, M. W. Jung*

School of Biological Sciences and Chemistry/Institute of Basic Science,
Sungshin Women's Univ., Seoul, 136-742, Korea,

* Corresponding author (mwjung@sungshin.ac.kr)

Keywords: *Alumina, Nickel, Sol-gel method, P123, hydrogen permeation*

1 Introduction

Ceramic-metal (cermet) composite membranes have been developed for a wide range of application. These composite membranes with high permeability and selectivity were interested in numerous area, such as hydrogen purification, fuel cell technology and membrane reactor processes. [1-2] Most of studies were carried out the effect of the interaction between hydrogen and a metal surface, such as Pd, Ni and Pt deposited on porous metal oxide supports. Nickel was known as good hydrogen dissociation catalyst and the merits of inorganic membranes. However, there are some disadvantages, such as hydrogen embrittlement and degradation.

Alumina, based on its fine particle size, high surface area and good catalytic activity, substantially has potential ceramic for several applications, such as an adsorbent, coating material, ceramic membrane, catalyst and its support. Porous alumina membrane is interested in membrane applications because it has high specific surface area and thermal stability. In order to improve the stability of membrane, metal oxide such as TiO_2, ZrO_2, NiO, etc were added to alumina and the stability of these membrane at higher temperatures were enhanced. [3-4] The NiO-doped Al_2O_3 catalysts had good activity at high temperature, so it makes improving thermal stability and the surface area.

NiO-doped Al_2O_3 powder was prepared by sol-gel technique. This process can change microstructure of homogeneous inorganic material precisely with controlling size and morphology of condensation materials.[5] There are several transition alumina by heat treatment and boehmite is one of the product of hydrolysis and condensation of water and aluminum alkoxide. It is transformed with changing temperatures through $\gamma \rightarrow \delta \rightarrow \theta \rightarrow \alpha$. The γ–Al_2O_3 among the transition alumina has especially high specific surface area, so it has been used as ceramic support. Moreover, it has the potential for broad application in catalyst supports and advanced ceramic owing to thermal and chemical stability with optical characteristics.

Similar to the mesoporous silicate, in all of these mesoporous alumina, the pore size and specific surface area is controlled by varying the size or concentration of surfactant molecules. Pluronic triblock P123 copolymer (Poly(ethylene oxide)20–poly(propylene oxide)70–poly(ethylene oxide)20) as surfactant has been used in the synthesis of mesoporous materials. As P123 was added during synthesis of alumina, it was used for increasing thermal stability and controlling morphology of grain. [6]

The purpose of this study was to make ceramic/metal composite membranes highly efficient and economic. It is to have these membranes that we synthesized by reducing the amount of metal and 20wt% NiO-doped Al_2O_3 powders with P123 by the sol-gel. The composite membranes were prepared by hot-press sintering as ceramic /metal materials and were proposed for their predominant hydrogen permeability and ability to maintain stability and mechanical properties at high operating temperatures. The hydrogen permeability of NiO-doped Al_2O_3/10wt% Ni membrane are measured and compared with previous paper of Al_2O_3/20wt% Ni sample. The reaction enthalpy was calculated by the Arrhenius plot. [7]

2 Experimental

2.1 Preparation of 20wt% NiO-doped Al_2O_3 powders

Aluminum isopropoxide ($Al(OC_3H_7)_3$) (CAS NO. 555-31-7, Aldrich) was dissolved in distilled water with a molar ration of $Al(OC_3H_7)_3$: H_2O=1:100 at 353K. 20wt% of $Ni(NO_3)_2 \cdot 6H_2O$ (CAS NO. 13478-00-7, Aldrich) to $Al(OC_3H_7)_3$ was added and refluxed for 3h. Nitric acid (HNO_3) as an acid catalyst was added to this reaction mixture for peptization to obtain homogeneous sol. 10wt% of P123 surfactant was used for the 20wt% NiO-doped Al_2O_3 powder with P123. These sol solutions were stirred overnight and stayed for 24h to get gel sample after quenching. These gel were washed with water and alcohol, followed by drying at 393 K for 24h. These powders were heat-treated from 773 K to 1473 K.

2.2 Preparation of NiO-doped Al_2O_3/Ni composite membranes

In order to obtain membrane specimens for hydrogen permeation, the mechanical alloying process was milled with a zirconia ball for 1h to mix a pure Ni (99.9%, Aldrich) metal and the synthesized powder with P123 heat-treated at 973 K with a weight ratio of 1:9. The consolidation of powder was performed using hot-press sintering (HPS). The heating rate and the pressure were 5 K/min and 808 MPa. Sintering was proceeded at 1473 K for 2 h under vacuum.

2.3 Characterization

Thermal degradation of the composites was measured using TG/DTA (NETZSCHSTA490PC, from room temperature to 1673K) with a heating rate of 276 K/min under air atmosphere. The structure change and phase transformation of the NiO-doped Al_2O_3 powder with and without P123 was characterized by X-ray diffraction measurements (XRD, Bruker D8 Focus, 40 kV, 40 mA, 0.2°/min, 10-80°) using CuKα radiation (λ = 1.5406 Å) The morphology and microstructure of these powders heat-treated at 973 K were analyzed by field-emission scanning electron microscopy (FE-SEM, JEOL-JMS 7500F). The specific surface area and pore size of these powders were measured by brunauer-emmett-teller surface analyzer (BET, BELSORP-mini).

2.4 Permeability experiments

The hydrogen permeation equipments consisted of a pressure controller, mass flow controller (MFC), permeation cell and stainless steel 0.25-inch-long tube that could withstand on high temperature for our experiments. The permeation-cell-equipped NiO-doped Al_2O_3/Ni membrane was placed in a furnace under controlled temperatures. The temperature was increased less than 5 K/min to prevent cracking of the membrane by rapid thermal difference, followed by being installed the membrane within furnace. The gas chromatograph (GC) was used for composition analysis of the permeated gas. Hydrogen concentration was measured by thermal conductivity detector (TCD) that analyzed the difference between hydrogen and nitrogen gas as carrier through thermal conductivity.

3 Results and discussion

The TGA and DTA curves of NiO-doped Al_2O_3 powders with and without P123 dried at 393K for 48h are shown in Fig. 1 (a) and (b) and both have similar diagram. The first weight loss around 473-673 K is because of the evaporation of remaining water and organic group in the reaction mixture. The amount of endothermic until 687.6 K ($\triangle H_{end}$ = 1.3 kJ/g) in (a) and 698 K ($\triangle H_{end}$ = 2.2 kJ/g) in (b) are for phase transformation to the γ–Al_2O_3. The exothermic peak was caused to the rearrangement of aluminum and oxygen ions in the alumina, and another one around 1073 K to 1373 K was attributed to γ phase formation.

Fig. 2 (a) and (b) show XRD patterns of heat-treated NiO-doped Al_2O_3 powders with and without P123 heat-treated at various temperatures. Main peaks of nickel aluminum oxide and weak peaks of γ–Al_2O_3 start to appear at 773 K. These broad peaks were continued until 1173 K and changed to sharp as increasing temperatures in (a) and (b). The γ–Al_2O_3 peaks (JCPDS file No. 50-0741, cubic, a = 0.8 nm, S.G = Fd-3m) were observed at the rate of 3.15% until 1373 K and were transformed to α–Al_2O_3 phases (JCPDS file No. 5-0712, Hexagonal, a = 0.5 nm, b = 0.5 nm, c = 1.3 nm) with very sharp peaks at the rate of 64.66% at 1473K. The diffraction peaks of $Ni_{0.94}Al_2O_{3.09}$ (JCPDS file No. 01-078-2180, cubic, a = 0.8 nm) were shown at the rate of 96.85% and 35.34% at 1373K and1473 K, respectively and were maintained to 1473 K with increasing.

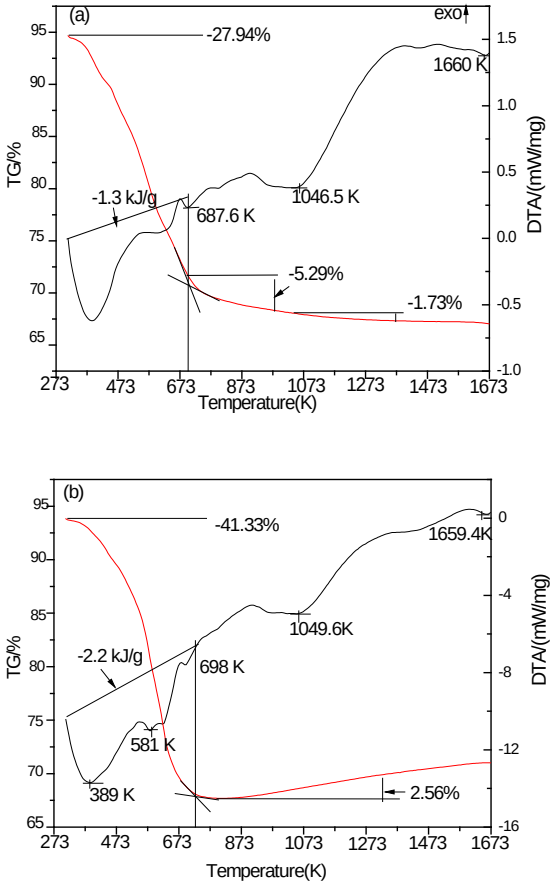

Fig. 1. TG-DTA curves of the NiO-doped Al_2O_3 powder (a) with (b) without P123

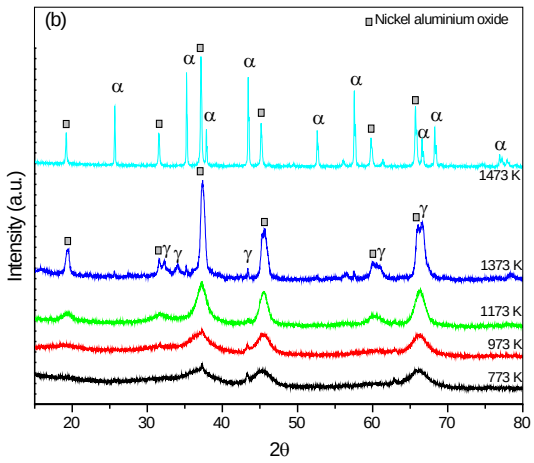

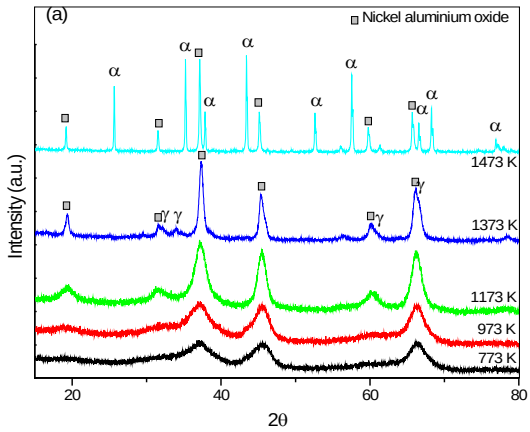

Fig. 2. XRD patterns of the NiO-doped Al_2O_3 powders (a) with (b) without P123 heat-treated at various temperatures.

Fig. 3 (a) shows nitrogen sorption isotherms of NiO-doped Al_2O_3 powder with and without P123 heat-treated at 973 K. All of two powders give typical type Ⅳ isotherms with a H_2 hysteresis loop as defined by IUPAC (International Union of Pure and Applied Chemistry). A type H_2 hysteresis loop is commonly associated with ink-bottle pores or voids between close-packed spherical particles. Comparing with both samples, powder with P123 have increased in total pore volume, indicating that pore diameter was mesoporous from analyzing S-shape of this diagram. Fig. 3 (b) indicated BJH (Barrett-Joyner-Halenda method) pore size distribution of NiO-doped Al_2O_3 powders. The average pore size was increased from 5.7 to 6.1 nm by adding P123.

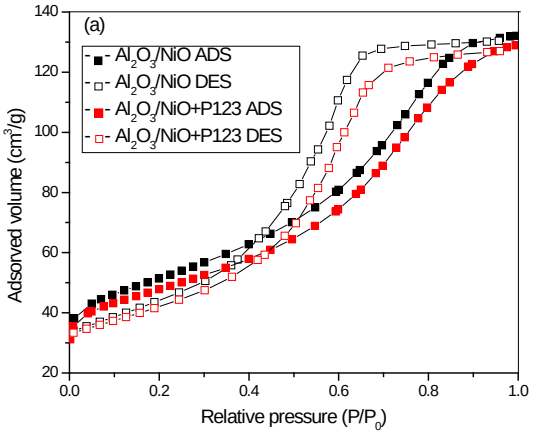

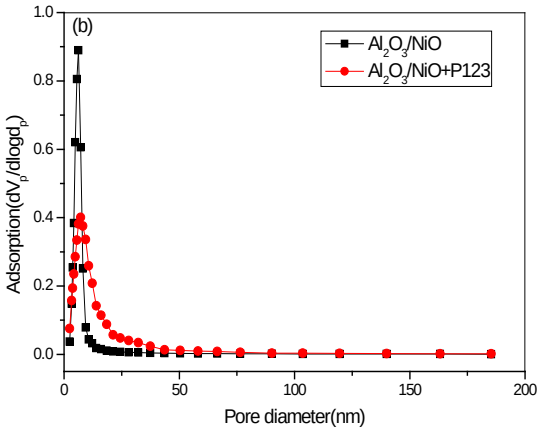

Fig. 3. (a) Nitrogen adsorption-desorption isotherms and (b) pore size distribution of the NiO-doped Al_2O_3 powders with and without P123 heat-treated at 973 K.

The surface morphology and surface area of NiO-doped Al_2O_3 powder with and without P123 are shown in Fig. 4. The surface was overlapped each other like aggregation with clustered rod shape in Fig. 4(b). The surface area with P123 were slightly larger than powder without P123 because it is expected to be improved surface area due to induced hydrogen bonding interaction between non-ionic block copolymer (P123) and Al species.

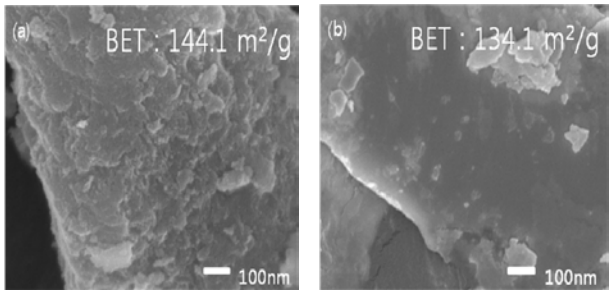

Fig. 4. FE-SEM micrographs and BET of the NiO-doped Al_2O_3 powders (a) with (b) without P123 heat-treated at 973 K.

Fig. 5 shows the XRD pattern for NiO-doped Al_2O_3/10wt% Ni composite membrane (a) before and (b) after hydrogen permeation testing. The diffraction patterns from Fig. 5 (a) and (b) were observed α-Al_2O_3 (JCPDS file No. 5-0712, Hexagonal, a = 0.5 nm, b = 0.5 nm, c = 1.3 nm), Ni metal (JCPDS file No. 03-1051, cubic, a = 0.6 nm) and $NiAl_2O_4$ (JCPDS file No. 10-0339, cubic, a = 0.8 nm) with sharp and strong intensity peaks. Especially, $NiAl_2O_4$ peaks of spinel structure were observed and it was considered as stable crystalline phases formed by the HPS process.

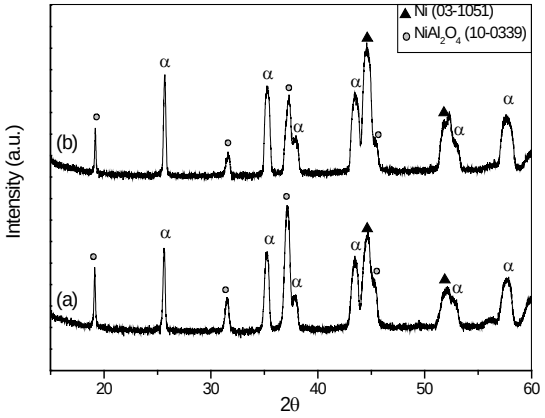

Fig. 5. XRD patterns of NiO-doped Al_2O_3-20wt% Ni membranes (a) before and (b) after the hydrogen permeation test.

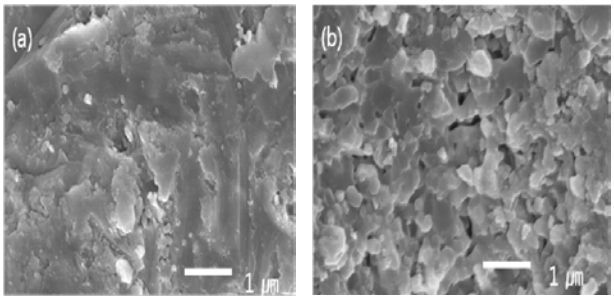

Fig. 6. FE-SEM photographs of the NiO-doped Al_2O_3 membrane surface (a) before and (b) after the hydrogen permeation test.

Fig. 6 shows SEM photographs of the surface morphology of the NiO-doped Al_2O_3/10wt% Ni composite membrane (a) before and (b) after hydrogen permeation test, respectively. It was seen from Fig. 6 (a) that the surface has dense state although the particle sizes were not homogeneous. By HPS, nickel powder was spread to pore result from sintering of NiO-doped Al_2O_3 at high temperature, increasing strength of ceramic-based membrane. The membrane expected to occur on surface diffusion mechanism such ad dense metallic membrane because its surface was dense different from other ceramic membrane. Fig. 6 (b) was NiO-

doped Al_2O_3/Ni composite membrane after evaluation of hydrogen permeation. After the test, hydrogen molecules were separated through grain boundary and porous.

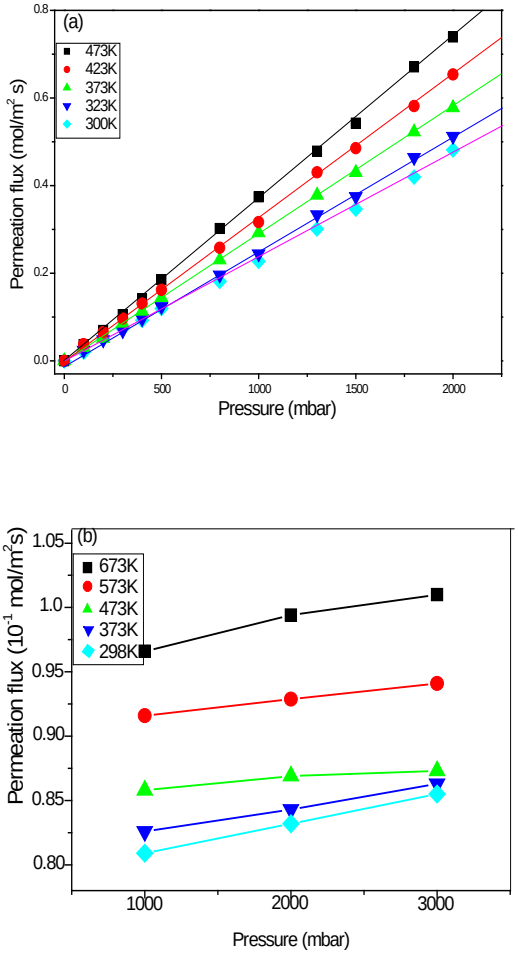

Fig. 7. Hydrogen permeation fluxes through pressures (a) Al_2O_3/20wt% Ni [11] and (b) NiO-doped Al_2O_3/10wt% Ni membrane.

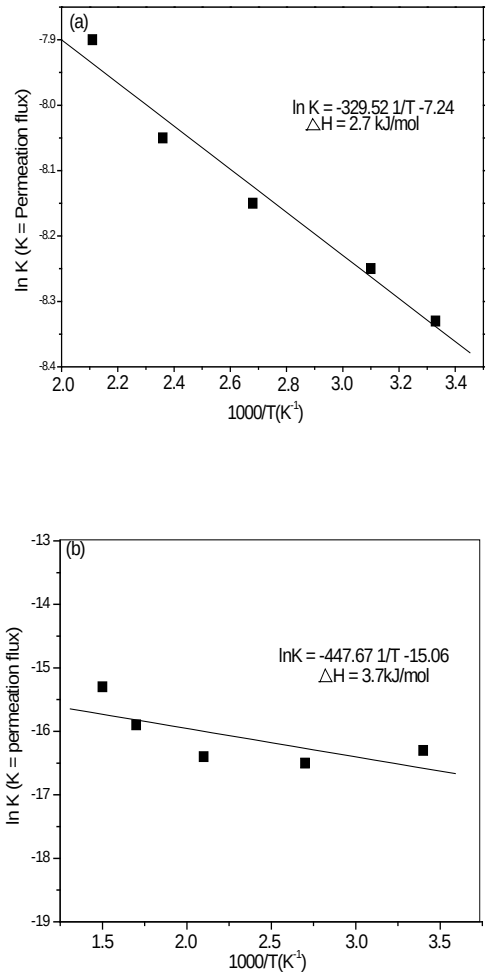

Fig. 8. Arrhenius's plots of the hydrogen permeability on (a) Al_2O_3/20wt% Ni [11] and (b) NiO-doped Al_2O_3 /10wt% Ni membrane.

Fig. 7 (a) shows the hydrogen permeation flux of the Al_2O_3-based membrane at 300, 323, 373, 423 and 473 K under increasing pressure with a range of 0.1, 0.3, 0.5, 0.8, 1.0, 1.3, 1.5, 1.8 and 2.0 bar [7] and the permeation test of (b) was at room temperature 298, 373, 473, 573 and 673K under increasing pressure with a range of 1.0, 2.0 and 3.0 bar. The hydrogen permeation flux increased with increasing temperature and differential pressure. This is consistent with the solution-diffusion mechanism of hydrogen. [8] The hydrogen permeation flux for the 20wt% NiO-doped Al_2O_3/10wt% Ni membrane obtained 0.087 mol/m^2 s at 473K. Although it was evaluated lower than Al_2O_3-20wt% Ni membrane (0.374 mol/m^2 s at

473K) [7], it was better than for the Ni/ceramic membrane (2.5 x 10^{-3} mol/m^2 s at 873K) [9] and Ni/BCZY cermet membrane (4.2 x 10^{-6} mol/m^2 s at 1173K) [10].

Fig. 8 shows the Arrhenius's plot for hydrogen permeation. Reaction enthalpy (ΔH) for the Al_2O_3-20wt% Ni and 20wt% NiO-doped Al_2O_3/10wt% Ni membranes was calculated to 2.7 kJ/mol and 3.7 kJ/mol. These results show that hydrogen permeation through membranes were measured by the endothermic reaction and dominated by gas pressure and reaction temperatures.

4 Conclusion

This work was conducted to investigate the hydrogen permeation of 20wt% NiO-doped Al_2O_3/10wt% Ni membrane under increasing pressure and temperature. The Al_2O_3 synthesized by sol-gel method was performed useful ceramic supports because it had high specific surface area and enhanced thermal stability at high temperature. The 20wt% NiO-doped Al_2O_3/10wt% Ni composite materials were prepared successfully by the HPS process and obtained excellent membrane with high hydrogen permeability about 0.1 mol/m^2 s at 673K.

Acknowledgments

This work was supported by the grants for professors of the Sungshin Women's university of 2011**.**

References

[1] T. Talebi, M. H. Sarrafi, M. Haji, B. Raissi and A. Maghsoudipour "Investigation on microstructures of NiO-YSZ composite and Ni-YSZ cermet for SOFCs". *Int. J. Hydrogen Energy*, Vol. 35, No. 17, pp 9440-9447, 2010

[2] T. M. Adams and J. Mickalonis "Hydrogen permeability of multiphase V-Ti-Ni metallic membranes", *Mater Lett*. Vol. 61, pp 817-820, 2007

[3] A. L. Ahmad and N. N. N. Mustafa "Sol-gel synthesized of nanocomposite palladium-alumina ceramic membrane for H_2 permeability: Preparation and characterization". *Int. J. Hydrogen Energy*, Vol.32, No. 12, pp 2010-2021, 2007

[4] N. Srisiriwat, S. Therdthianwong and A. Therdthianwong "Oxidative steam reforming of ethanol over $Ni/_Al_2O_3$ catalysts promoted by CeO_2, ZrO_2 and CeO_2-ZrO_2", *Int. J. Hydrogen Energy*, Vol. 34, pp 2224-2234, 2009

[5] J. Li, X. Wang, L. Wang, Y. Hao, Y. Huang, Y. Zhang et al. "Preparation of alumina membrane from aluminum chloride", *J. Membr. Sci*., Vol. 275, No. 1-2, pp 6-11, 2006

[6] F. Huang, Y. Zheng, G. Cai, Y. Zheng, Yigong and K. Wei "A new synthetic procedure for ordered mesoporous γ-alumina with a large surface area". *Scripta Materialia*, Vol. 63, No. 3, pp 339-342, 2010

[7] J. H. Park, T. W. Hong and M. W. Jung "Hydrogen permeation on Al2O3-based nickel/cobalt composite membranes". *Int. J. Hydrogen Energy*, Vol. 35, pp 12976-12980, 2010

[8] J. Shu, B. P. A. Grandjean, A. van Neste, S. Kaliaguine "Catalytic palladium-based membrane reactors". *Can. J. Chem. Eng*. Vol. 69, pp1036-1060, 1991

[9] B. Ernst, S. Haag and M. Burgard " Permselectivity of a nickel/ceramic composite membrane at elevated temperatures : a new prospect in hydrogen separation?". *J. Membr. Sci*. Vol.288, No. 1-2, pp 208-217, 2007

[10] L. Yan, W. Sun, L. Bi, S. Fang, Z. Tao and W. Liu "Influence of fabrication process of Ni-$BaCe_{0.7}Zr_{0.1}Y_{0.2}O_{3-\delta}$ cermet on the hydrogen permeation performance". *J. Alloys Compd*. Vol. 508, pp L5-L8, 2010